

FIG. 3. Fit to the Dalitz-plot distribution in terms of  $\xi(0)$  and  $\lambda_+$ . The contours show the loci where the  $\chi^2$  probability is less than the maximum probability by the factors indicated. Results of other analyses are also shown. These are discussed in the text.

the summary of Gaillard and Chounet of the whole previous  $K_{\mu 3}^+$  decay distribution results, derived mainly from the work of Kijewski *et al.*<sup>3</sup> and D. Haidt *et al.*,<sup>4</sup>  $\xi(0) = -1.00 \pm 0.40$  and  $\lambda_+ = 0.043 \pm 0.017$ ; the summary derived from all previous

$K_{\mu 3}^+$  experiments,  $\xi(0) = -0.85 \pm 0.20$ ,  $\lambda_+ = 0.017 \pm 0.008$ ; and the summary of all  $K_{13}$  data,  $\xi(0) = -0.65 \pm 0.20$  and  $\lambda_+ = 0.034 \pm 0.006$ . It is desirable to consider the results from various classes of analyses separately, as differences in the values of the parameters so calculated would indicate violations of the usual premises of weak-interaction calculations such as  $\mu$ - $e$  universality, the absence of second-class currents and the locality of weak interactions. We note that our present results are closer to the best fit to all previous data on the decay correlations in  $K_{\mu 3}^+$  decays.

We wish to express our appreciation for the assistance and cooperation of the Argonne National Laboratory staff. Dr. Irwin Spirn was primarily responsible for the design and construction of the separated  $K$ -meson beam, and we are very much indebted to Dr. Spirn for his invaluable contributions to the operation of the beam throughout the experiment.

\*Work performed under the auspices of the U. S. Atomic Energy Commission.

†Now at Indiana University, Bloomington, Ind. 47401.

‡Now at Cornell University, Ithaca, N. Y. 14850.

<sup>1</sup>M. K. Gaillard and L. M. Chounet, CERN Theoretical Studies Report No. CERN 70-14, 1970 (unpublished). This is an invaluable review of theoretical (by M.K.G.) and experimental (by L.M.C.) work on  $K_{13}$  decays.

<sup>2</sup>S. W. MacDowell, *Nuovo Cimento* **6**, 1445 (1957).

<sup>3</sup>P. K. Kijewski *et al.*, UCRL Report No. 18433, 1969 (unpublished).

<sup>4</sup>D. Haidt *et al.* (X2 Collaboration), *Phys. Lett.* **29B**, 691 (1969).

## Reaction $\pi^+ p \rightarrow \rho^+ p$ at 2.67 GeV/c: A Study of Isoscalar Exchanges\*

W. Michael and G. Gidal

Lawrence Berkeley Laboratory, University of California, Berkeley, California 94720

(Received 22 March 1972)

Results are presented of a study of the reaction  $\pi^+ p \rightarrow \rho^+ p$  at 2.67 GeV/c incident  $\pi^+$  momentum. The contributions due to given spin-parity exchanges are isolated; and, by combining these results with those of a similar  $\pi^-$  experiment, the  $I_4 = 0$  component of each series is separated. The  $\omega$  ( $I=0, J^{PC}=1^{--}$ ) exchange contribution shows a pronounced dip at  $-t=0.4$  (GeV/c)<sup>2</sup>. Evidence is presented for the exchange of a state of minimum quantum numbers,  $H$  ( $I=0, J^{PC}=1^{+-}$ ).

This Letter reports the results of a high-statistics hydrogen-bubble-chamber experiment to study the reaction  $\pi^+ p \rightarrow \rho^+ p$  at an incident  $\pi^+$  momentum of 2.67 GeV/c.<sup>1</sup> A sample of some 9500

events of the reaction  $\pi^+ p \rightarrow \pi^+ p \pi^0$  has been obtained from a 300 000-picture exposure of the 25-in. hydrogen bubble chamber at the Bevatron. The events were measured on the flying spot dig-

itizer, and in addition to conventional kinematic fitting, the automatically obtained ionization information has been used to aid in the separation of hypotheses.<sup>2</sup> The Dalitz plot of the events assigned to  $\pi^0$  production shows that this reaction is dominated by the quasi-two-body final states  $\rho^+p$ ,  $\Delta^{++}\pi^0$ , and  $\Delta^+\pi^+$ , and also exhibits smaller amounts of final states involving higher-mass  $N^*$ 's and diffractive dissociation of the proton.

A maximum-likelihood fit has been made to determine the amounts and parameters of each of the several identifiable processes.<sup>3</sup> The events have been fitted with a distribution of the form  $D = \sum b_k w_k + \Phi$ , where for the  $k$ th process,  $b_k$  is a Breit-Wigner line shape, of given orbital angular momentum, for which the mass and width were allowed to vary for the major processes;  $w_k$  is the  $s$ -channel helicity decay distribution whose parameters (the spin-density-matrix elements) were allowed to vary for the major processes; and  $\Phi$  is a constant representing phase space.<sup>4</sup> The amount of "phase-space" background  $\Phi$  is found by this fit to be 0. Some 50% of the events are attributed to  $\rho^+$  production. This corresponds to a total cross section for  $\rho^+$  production of  $1.40 \pm 0.08$  mb.

To determine the physical parameters as a function of four-momentum transfer to the proton,  $t$ , the domain of  $t$  was first subdivided into "coarse" intervals and a fit using all identified processes (from the fit to the full domain) was made for each interval. Any process not contributing in a given interval was excluded from the distribution for further fits within that interval. The intervals were then subdivided into finer bins and another fit performed. The results for the differential production cross section of  $\rho^+$  and its spin-density-matrix elements are presented in Figs. 1(a)–1(c). The density-matrix elements in the  $t$ -channel helicity (or Gottfried-Jackson) frame were calculated from the moments of all events (in a given  $t$  bin) weighted according to their probability of resulting from  $\rho^+$  production as found by the maximum-likelihood fit (in the  $s$ -channel). The values obtained are shown in Figs. 1(d)–1(f).

By making appropriate linear combinations of the density-matrix elements, it is possible to isolate, to order  $1/s$ , the contribution to the cross section of the exchange of a given spin-parity series as follows<sup>5</sup>: (1)  $\rho_{00} \frac{d\sigma}{dt}$ , which measures meson helicity-nonflip unnatural parity exchange, (2)  $(\rho_{11} - \rho_{1-1}) \frac{d\sigma}{dt}$ , which measures meson helicity-flip unnatural parity exchange,

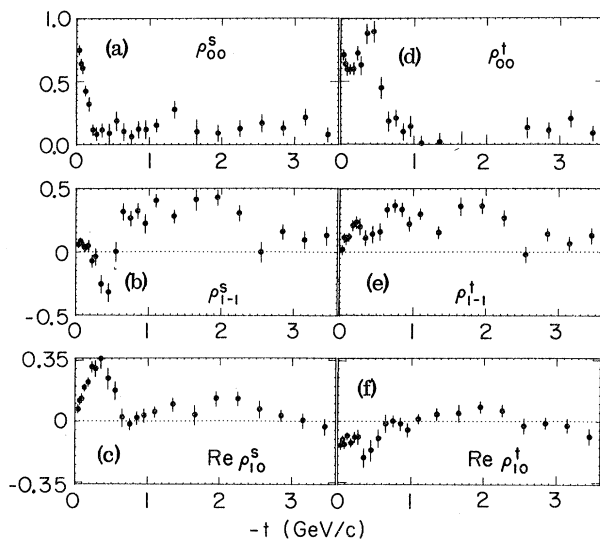


FIG. 1. Spin-density-matrix elements of the  $\rho^+$  produced in  $\pi^+p \rightarrow \rho^+p$  at 2.67 GeV/c. Superscripts indicate the channel in which the  $\rho$  helicity is measured.

and (3)  $(\rho_{11} + \rho_{1-1}) \frac{d\sigma}{dt}$ , which measures natural parity exchange (necessarily meson helicity flip). Graphs of these products in the  $t$ -channel helicity frame are shown in Figs. 2(d)–2(f). Also shown in Figs. 2(b) and 2(c) are the product (1) and the product  $\text{Re} \rho_{10} \frac{d\sigma}{dt}$  in the  $s$ -channel helicity frame.

These results show a number of striking features:

(i) The differential cross section [Fig. 2(a)] has a sharp forward peak, a dip at  $-t \approx 0.4$ , a broader second maximum, and a second minimum at  $-t \approx 1.6$ .<sup>6</sup>

(ii) The natural-parity-exchange contribution [product (3), Fig. 2(d)] shows a turnover in the very forward direction, a pronounced dip at  $-t \approx 0.4$ , and a suggestion of a dip at  $-t \approx 1.6$ . The minimum quantum numbers for this contribution should be represented by  $\omega$  ( $I = 0, J^{PG} = 1^{-}$ ) and  $A_2$  ( $I = 1, J^{PG} = 2^{+-}$ ).

(iii) The nonflip unnatural-exchange contribution [product (1), Fig. 2(e)] falls off smoothly from a strong forward peak, showing no evidence of any structure below  $-t \approx 1.0$ . On the other hand,  $\rho_{00}^t$  [Fig. 1(d)] drops from a value of about 0.7 in the forward direction, rises to about 0.9 at  $-t \approx 0.4$ , and then decreases smoothly with increasing momentum transfer. This shows that nonflip unnatural parity exchange accounts for some 90% of the cross section at the first dip in  $d\sigma/dt$ . The  $\pi$  and a  $1^+$  object, e.g.,  $A_1$  or  $H$ , should represent the minimum quantum numbers

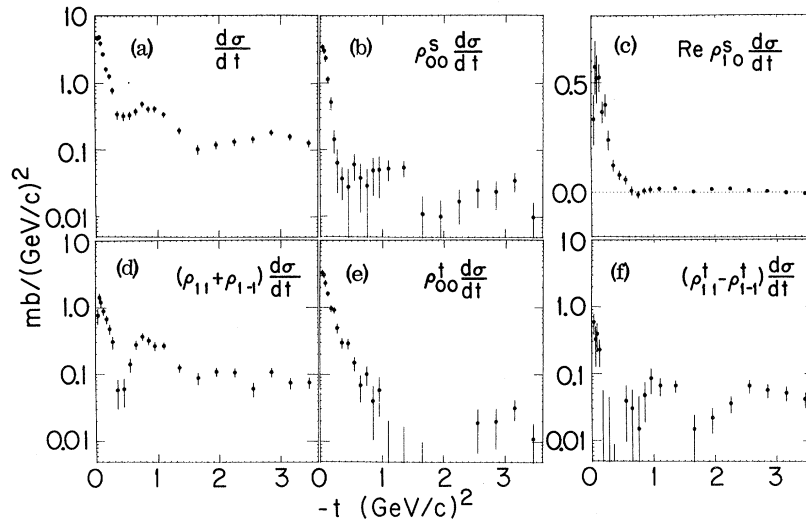


FIG. 2. (a) Differential cross section for  $\pi^+p \rightarrow \rho^+p$  at 2.67 GeV/c. (b)–(f) Products of the differential cross section with pertinent combinations of spin-density-matrix elements.

for this contribution.

(iv) The helicity-flip unnatural-parity contribution [product (2), Fig. 2(f)] shows a sharp forward spike, and some discontinuity at  $-t \approx 1.6$ . Again,  $A_1$  or  $H$  should represent the minimum quantum numbers for this contribution.

(v) In both  $s$ - and  $t$ -channel helicity frames,  $\text{Re}\rho_{10}$  has significantly nonzero values. In the  $t$  channel [Fig. 1(f)] it starts at negative values near  $-t=0$  and rises to zero at  $-t \approx 0.65$ . Examination of the  $t$ -channel helicity amplitudes shows that these nonzero values of  $\text{Re}\rho_{10}^t$  imply the presence of nonzero-spin unnatural parity exchanges (i.e., minimum  $J^P = 1^+$ ). This observed behavior of  $\text{Re}\rho_{10}^t$  is essentially identical to that observed in  $\rho^-$  production,<sup>7,8</sup> and since in particular the sign is the same, it indicates that the interference is among isoscalar exchanges. In the  $s$  channel [Fig. 1(c)]  $\text{Re}\rho_{10}^s$  reaches its maximum allowed value near  $-t \approx 0.3$ , then drops to zero at  $-t \approx 0.65$ . The product  $\text{Re}\rho_{10}^s d\sigma/dt$ , [Fig. 2(c)] also first reaches zero at  $-t \approx 0.65$ .

(vi) The product  $\rho_{00}^s d\sigma/dt$  [Fig. 2(b)] drops very sharply from a forward peak, then remains approximately constant to beyond  $-t=1$ . Strong-cut models of this reaction have predicted a dip in this quantity at  $-t \approx 0.5$  and a corresponding zero in  $\text{Re}\rho_{10}^s d\sigma/dt$ . In wrong-signature nonsense-zero (WSNZ) models this structure would be expected closer to  $-t=1$ , but the introduction of weak cuts could modify this prediction.

Additional information may be obtained by combining these results with those of a similar high-statistics bubble-chamber experiment using a

beam of  $\pi^-$ 's at 2.77 GeV/c in which the reactions  $\pi^-p \rightarrow \rho^-p$  and  $\pi^-p \rightarrow \rho^0n$  were studied.<sup>7</sup> Appropriate linear combinations of the differential cross sections and the products (1)–(3) for  $\rho^\pm$  and  $\rho^0$  production serve to separate the isospin components of that quantity.<sup>9</sup> Since the  $I_t=1$  component of the amplitude changes sign under charge conjugation while the  $I_t=0$  component does not, the isoscalar,  $T_0$ , and isovector,  $T_1$ ,  $t$ -channel amplitudes appear in the combinations  $T_0 \mp T_1$  for  $\rho^\pm$  production and  $\sqrt{2}T_1$  for  $\rho^0$  production. Hence, the  $I_t=0$  component of a quantity  $X$  is given by  $X_0(t) = \frac{1}{2}[X^+(t) + X^-(t) - X^0(t)]$ , and the  $I_t=1$  component by  $X_1(t) = \frac{1}{2}X^0(t)$ , where  $X^\pm$  and  $X^0$  are the corresponding quantities for the reactions producing  $\rho^\pm$  and  $\rho^0$ , respectively. Similarly, the relative phase  $\delta$  between the isoscalar and isovector exchange components is given by  $\cos\delta(t) = [X^-(t) - X^+(t)]/4[X_0(t)X_1(t)]^{1/2}$ . The  $I_t=0$  contributions to the differential cross section and the products (1)–(3) are shown in Figs. 3(a)–3(d). The cosines of the relative isoscalar and isovector phases for the differential cross section and the products (1) and (2) are shown in Figs. 3(e)–3(g). The density-matrix element  $\text{Re}\rho_{10}^t|_{t=0}$  defined as  $X_0(\text{Re}\rho_{10}^t d\sigma/dt)/X_0(d\sigma/dt)$ , is plotted in Fig. 3(b).<sup>10</sup>

Some salient features of these results are:

(I) The  $I_t=0$  differential cross section [Fig. 3(a)] shows structure similar to that observed for natural parity exchange above, especially the sharp dip at  $-t \approx 0.4$ . Such a dip in  $X_0(d\sigma/dt)$  has been reported previously.<sup>9,11</sup>

(II) The  $I_t=0$  natural parity contribution [Fig.

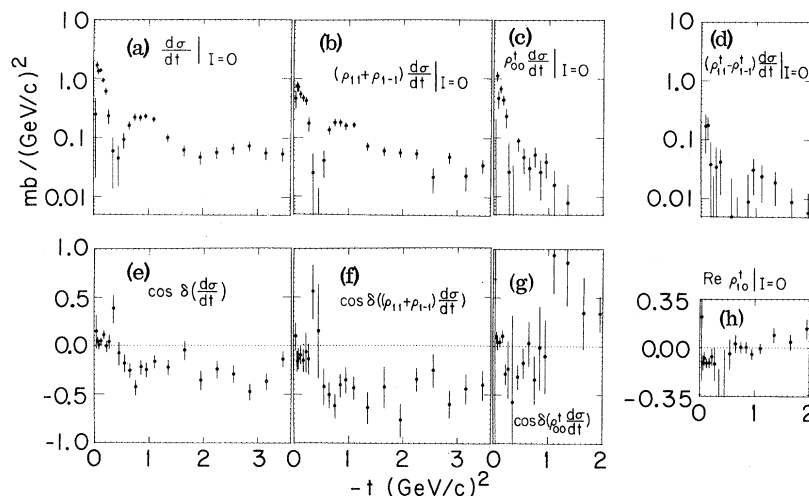


FIG. 3. (a)–(d) Isoscalar components of the differential cross section and particular spin-parity contributions. (e)–(g) Cosine of the relative phase to (a)–(c). (h) Isoscalar density-matrix element  $\text{Re} \rho_{10}^t$  [compare Fig. 1(f)].

3(b)] shows this same dip structure (and in fact is consistent with zero at  $-t \approx 0.4$ ) indicating the source of this structure as a system having the quantum numbers of the  $\omega$  meson. In a WSNZ Regge model this would fix the zero of the  $\omega$  trajectory at  $-t = 0.4 \pm 0.05$ . Together with the  $\omega$  mass this implies a trajectory  $\alpha_\omega(t) = 0.4 + t$ , lying somewhat lower than the commonly accepted  $\rho$  trajectory.

(III) The  $I_t = 0$  nonflip unnatural-exchange contribution [Fig. 3(c)] shows a strong forward peak, representing about one half the total forward peak in  $I_t = 0$ . This must be explained by the presence of an effective exchange having minimum quantum numbers  $I=0$ ,  $J^{PG} = 1^{+-}$ , e.g., the  $H$  meson or a  $\pi$ - $\rho$  Regge-Regge cut. Likewise the  $I_t = 0$  component of  $\text{Re} \rho_{10}^t$  [Fig. 3(h)] can be nonzero only if such a state is present. The presence of such a state would also be sufficient to account for the observed behavior of  $\text{Re} \rho_{10}^t$  for the  $\rho^+$  data alone [compare Figs. 1(f) and 3(h)]. The  $I_t = 0$  helicity-flip unnatural-exchange component [Fig. 3(d)], which to order  $1/s$  measures this same state, is nonzero in the same region of momentum transfer.

(IV) The cosine of the relative phase between isoscalar and isovector exchanges can serve to indicate exchange degeneracy in a given spin and parity series, since this cosine will be zero for exchange-degenerate states. The converse statement is not generally true, but is essentially true in particular cases.<sup>12</sup> For the natural series, representing  $\omega$  and  $A_2$ , this cosine [Fig. 3(f)] is consistently nonzero (negative). For the unnatural series, representing predominantly  $\pi$  and  $H$ ,

this cosine [Fig. 3(g)] is consistent with zero in the region of significant  $H$  signal, an indication that the  $H$  is exchange degenerate with the pion.

In summary, the natural-parity exchange contribution to  $\rho^+$  production has features generally associated with  $\omega$  exchange, and this is confirmed by separation of the  $I_t = 0$  component. The unnatural-parity contribution shows features generally associated with  $\pi$  exchange, but nonzero values of  $\text{Re} \rho_{10}^t$  indicate the presence also of nonzero-spin unnatural parity exchanges. This is confirmed by separation of the  $I_t = 0$  component, where a strong signal is seen in  $X_0(\rho_{00} d\sigma/dt)$ . This can be explained only by the presence of a state of minimum effective quantum numbers,  $H$  ( $I=0$ ,  $J^{PG} = 1^{+-}$ ).

The authors wish to thank Dr. Gary Goldstein, Dr. Donald Grether, and Mr. Fred Lott for many illuminating discussions.

\*Work done under the auspices of the U. S. Atomic Energy Commission.

<sup>1</sup>A preliminary account of this experiment is presented in *Particles and Fields, AIP Conference Proceedings No. 2*, edited by A. C. Melissinos and P. F. Slattery (American Institute of Physics, New York, 1971).

<sup>2</sup>The program HAZE with ionization and FOG-CLOUDY-FAIR were used to process the events.

<sup>3</sup>P. Eberhard and W. Koellner, UCRL Report No. UCRL-20159, 1970 (unpublished).

<sup>4</sup>K. Gottfried and J. D. Jackson, *Nuovo Cimento* **33**, 309 (1964); J. D. Jackson, *Nuovo Cimento* **34**, 1644 (1964). The results for the differential cross section and density-matrix elements are, however, quite insensitive to the precise choice for the Breit-Wigner

line shape.

<sup>5</sup>Gottfried and Jackson, Ref. 4; J. P. Ader, M. Capdeville, G. Cohen-Tannoudji, and Ph. Salin, *Nuovo Cimento* **56A**, 952 (1968); D. Grether, unpublished.

<sup>6</sup>No correction has been made for a possible small scanning loss in the forward bin [ $-t \in (0.025-0.050)$ ], since it is not necessary within the scope of this Letter, and its precise determination is rather costly. The maximum reasonable correction, however, would not change the qualitative aspect of any result involving that bin.

<sup>7</sup>J. Bonchez, G. Laurens, J. P. Baton, and F. Cadiet, to be published; J. P. Baton and G. Laurens, *Nucl. Phys.* **B21**, 551 (1970).

<sup>8</sup>D. H. Miller *et al.*, *Phys. Rev.* **153**, 1423 (1967).

<sup>9</sup>A. P. Contogouris, J. Tran Than Van, and H. J. Lubatti, *Phys. Rev. Lett.* **19**, 1352 (1967).

<sup>10</sup>In computing the results of Fig. 3, a small correc-

tion ( $\approx 7\%$ ) has been applied to the overall normalization of the  $\pi^-$  experiment, to account for the slight difference in beam momentum of the two experiments. This correction was taken from a power-law fit to all available data for this reaction [CERN Reports No. CERN-HERA 70-7, and No. 70-5, 1970 (unpublished)]. The sensitivity of these results to the normalization was checked by varying the relative normalization of the two experiments by  $\pm 20\%$ . In no case did the points plotted in Figs. 3(a)-3(b) change by more than one standard deviation. [Both experiments are within less than 20% of the power-law fits for their respective charges. A power-law fit by the authors to more recent results, including that of this experiment, gives  $\sigma(\pi^+p \rightarrow \rho^+p) = (9.6 \pm 0.9)P_{\text{lab}}^{-1.98 \pm 0.06}$ .]

<sup>11</sup>D. J. Crennell *et al.*, *Phys. Rev. Lett.* **27**, 1674 (1971).

<sup>12</sup>G. R. Goldstein, private communication.

## Electron Spin Motion in a Magnetic Mirror Trap

Sara Granger and G. W. Ford

*Department of Physics, University of Michigan, Ann Arbor, Michigan 48104*

(Received 3 March 1972)

Averaging methods are used to discuss the electron spin motion in a magnetic mirror trap of the sort used in precision  $g-2$  experiments. An expression is obtained for the difference frequency correct up to second order in the field nonuniformity. When applied to the experiments this result removes the discrepancy between the last two precision  $g-2$  measurements and yields a corrected value for the gyromagnetic anomaly:  $a = (1\,159\,656.7 \pm 3.5) \times 10^{-9}$ .

In precision  $g-2$  experiments<sup>1,2</sup> electrons are confined in a weak magnetic mirror trap, i.e., a nearly uniform axially symmetric magnetic field which increases in strength on either side of a median plane. The electron's motion is a superposition of a rapid rotation (cyclotron motion) about the symmetry axis and a much slower longitudinal oscillation along the axis. The experiments measure the difference frequency  $\omega_D$  which is the long-time average precession rate of the electron's spin relative to its velocity. Previous analyses of these experiments have used a theoretical expression for  $\omega_D$  obtained by time averaging the uniform-field result over the field in the trap,<sup>1</sup> a procedure which is not in general correct. Here we give a perturbation expansion for  $\omega_D$ , obtained using averaging methods, correct up to second order in the field nonuniformity. We then apply this result to the last two precision  $g-2$  measurements to obtain corrected values for the gyromagnetic anomaly.

Choosing the field symmetry axis as the  $z$  axis,

the magnetic field in the trap is of the form

$$\vec{B}(\vec{r}) = B_0[\hat{z} + \vec{b}(\vec{r})], \quad (1)$$

where  $\vec{b}$  represents the small perturbation of the uniform field. The electron's orbital equations of motion are

$$d\vec{r}/dt = \vec{v}, \quad d\vec{v}/dt = \vec{\omega} \times \vec{v}, \quad (2)$$

where  $\vec{\omega} = e\vec{B}/\gamma mc$  with  $\gamma = (1 - v^2/c^2)^{-1/2}$ . Since the experiments measure the spin relative to the velocity, it is appropriate to write the spin equations of motion in a coordinate system in which  $\vec{v}$  is fixed, i.e., one rotating with instantaneous angular velocity  $\vec{\omega}$ . The resulting equation is

$$d\vec{S}/dt = \vec{\Omega} \times \vec{S}, \quad (3)$$

where<sup>3</sup>

$$\vec{\Omega} = a[\gamma(\vec{\omega} - \hat{v} \cdot \vec{\omega} \hat{v}) + \hat{v} \cdot \vec{\omega} \hat{v}], \quad (4)$$

with  $a$  the gyromagnetic anomaly. In general  $\vec{\Omega}$  is time dependent through the dependence of  $\vec{B}$ , and hence  $\vec{\omega}$ , upon electron position.